JOURNAL OF MATERIALS SCIENCE 15 (1980) 2296–2306

Effects of pre-strain on plane stress ductile fracture in α-brass

Y.W.MAI, B. COTTERELL
Department of Mechanical Engineering, University of Sydney, Sydney, N.S.W. 2006 Australia

The effects of pre-strain on plane stress ductile fracture in a 70/30 alpha brass Austral 207 have been studied using the deep-edge-notched tension (DENT) specimens. The amount of pre-strain varies between 5 and 35%. It is found that both the specific essential work of fracture (w_e) and the critical crack opening displacement (δ_c) decrease with increasing pre-strain. A simple theory for estimating the specific essential work of fracture in the presence of pre-strain is suggested and it gives good agreement with experimental results. Elongations to fracture in the DENT specimens are also predictable from a simple deformation analysis which considers the plastic elongations due to crack initiation, crack propagation and final stretch of a ligament that has reached a necking strain equal to that in a simple plain tension test. Micro-hardness measurements show that the strain localization is more intense near the fracture surface as the pre-strain level is increased and this is suggested to be an explanation for the low δ_c values obtained in pre-strained specimens.

1. Introduction

The study of pre-strain effects on the fracture behaviour of thin metal sheets is of practical significance. There are many metal forming and removal processes, such as stretching and deep drawing of plates, cold-punching of holes and guillotining of thin sheets, which involve cold-work. Knott and his co-workers [1, 2] have studied in some detail the effects of pre-strain in relatively thick metal bars and plates in which plane strain conditions prevail. In one study [1] they found that the crack opening displacements at crack initiation and at maximum load were smaller than those obtained for the normalized condition because of the low work hardening rate and high flow stress in the pre-strained specimens. Pre-strain also promotes shear lip formation on well-defined shear planes as opposed to the uniform extension and necking of a ligament in the normalized material. In another study [2] it was shown that the effect of pre-strain in ductile notched specimens was to vary the hydrostatic component of the triaxial stress state at the notch tip and to enhance lateral expansion of microvoids. Not all these experimental findings are applicable to thin metal sheets which are predominantly under plane stress conditions. For example there is little triaxial stress in thin sheets and pre-strain cannot appreciably alter the triaxial stress state.

In a previous paper [3] one of us has studied the specific essential work of fracture (w_e), i.e. the work that is dissipated in the end region containing the fracture process zone, for a low carbon (~ 0.1% C) sheet steel in both the as-received and strain-aged conditions. The effect of pre-strain on w_e was also investigated and it was concluded that the amount of pre-strain did not have any significant effects. The reason was thought to be a result of the material, whether pre-strained or not, entering the fracture process zone must have received the same total strain. In metals with low strain hardening rates, such as the low carbon steel studied in [3], this may be the case since the work dissipated up to necking is only a small fraction of w_e. However in other metals, such as copper, brass and normalized steels where the work hardening rate is large, pre-strain can have considerable effects on w_e. The purpose of the present paper therefore is to study the effects of pre-strain on the plane stress ductile fracture behaviour of a 70/30 alpha brass

 0022–2461/80/092296–11$03.10/0

and to show theoretically how w_e can be estimated when the amount of pre-strain is known.

2. Effect of pre-strain on specific essential work of fracture

The specific essential work of fracture (w_e) may be considered as that work dissipated in the fracture process zone at the crack tip and for a given sheet thickness is a material constant. This includes the plastic work up to necking in the material that is to form the process zone (w_{e1}) and the work to fracture the neck (w_{e2}). It is assumed that the fracture initiates when the crack opening displacement reaches a critical value δ_c.

Since there is uniform straining up to necking

$$w_{e1} = d\int_0^{\bar{\epsilon}_n} \bar{\sigma} d\bar{\epsilon} \quad (1)$$

where d is the width of the undeformed sheet that later forms the process zone, $\bar{\epsilon}_n$ the true strain at necking and the true stress ($\bar{\sigma}$)–true strain ($\bar{\epsilon}$) relationship is assumed to be

$$\bar{\sigma} = \kappa \bar{\epsilon}^n, \quad (2)$$

in which κ is a material constant and n is the work hardening rate. After necking, the deformation in the process zone is localized and non-uniform. Fracture occurs in the neck when the crack tip is further stretched to δ_c so that

$$w_{e2} = \int_{\epsilon_n d}^{\delta_c} \sigma(\delta) d\delta \quad (3)$$

where σ and ϵ_n are the engineering stress and strain at necking respectively. The functional dependence of σ on δ after necking can be obtained from tension specimens with shallow notches to force necking normal to the applied stress.

Using Equations 1 to 3, the specific essential work of fracture (w_e) can be expressed as

$$w_e = d\int_0^{\bar{\epsilon}_n} \kappa \bar{\epsilon}^n d\bar{\epsilon} + \int_{\epsilon_n d}^{\delta_c} \sigma(\delta) d\delta. \quad (4)$$

When the metal sheet has received a given amount of pre-strain ($\bar{\epsilon}_s$) the effect is to reduce w_{e1} by changing the lower limit to $\bar{\epsilon}_s$. Tensile pre-strain does not affect w_{e2}. Experiments on shallow-notched tension specimens (see section 5.2) show that the elongation ($\delta_c - \epsilon_n d$) necessary to fracture the neck after it has formed is independent of the degree of pre-strain. Pre-strain introduced by a manufacturing process such as rolling or deep drawing imparts additional anisotropy into the material to affect the neck deformation and δ_c. Thus for tensile pre-strain, the specific essential work ($_s w_e$) is given by

$$_s w_e = d\int_{\bar{\epsilon}_s}^{\bar{\epsilon}_n} \kappa \bar{\epsilon}^n d\bar{\epsilon} + \int_{\epsilon_n d}^{\delta_c} \sigma(\delta) d\delta \quad (5)$$

As the pre-strain $\bar{\epsilon}_s$ approaches the strain $\bar{\epsilon}_n$ at which necking initiates, the specific essential work term w_{e1} tends to zero. If one is presented with such a material without being told its prior history, it would be regarded as a material with a low work hardening rate [1] with $w_{e1}/w_e \ll 1$. A cold rolled low carbon steel, which corresponds to such a material, was previously studied by one of the authors [3]. For this material the true stress–true strain relationship is

$$\bar{\sigma} = 465\ \bar{\epsilon}^{0.10}\ \text{MPa} \quad (6)$$

and $d \approx 1.2$ mm, $\sigma(\delta) \approx \sigma_{UTS} = 400$ MPa and $\delta_c = 0.73$ mm. Equation 4 may be used to estimate w_e which gives $w_{e1} = 40$ kJ m^{-2} and $w_{e2} = 244$ kJ m^{-2} so that $w_e = 284$ kJ m^{-2} which is in good agreement with the experimental measurement of 275 kJ m^{-2} [3]. Note that w_{e1} is only 14% of w_e and when a pre-strain of 12% is present w_{e1} becomes zero. Thus the conclusion drawn in [3] that pre-strain does not affect w_e, in broad terms and within experimental limits, is valid for the particular steel studied. However this statement is not true in general and for the α-brass studied in the present work w_e depends on pre-strain.

3. Deformation and fracture of the deep edge notched tension specimen

The deep-edge-notched tension (DENT) specimen, Fig. 1, is a useful geometry for experimental measurement of the specific essential work of fracture for thin sheet metals [3, 4]. Since the elementary fracture theory of the DENT specimen was first presented by Cotterell and Reddel [4], considerable refinements have been made and a more detailed analysis on the deformation and fracture mechanics will be presented elswhere [5]. For the purpose of the present paper only relevant parts of the new analysis are given below.

3.3. Deformation theory

Regarding the deformation of the DENT specimen several assumptions have to be made: (1) Before crack initiation (δ) at the notch tip is equal to the plastic elongation (e) measured by the clip gauges

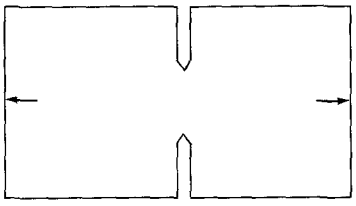

Figure 1 The deep-edge-notched tension (DENT) specimen.

(2) Crack initiation occurs when $\delta = \delta_c$ and the crack opening displacement at the tip of a propagating crack is a constant and equal to δ_c. (3) Necking occurs when the longitudinal strain reaches a critical value $\bar{\epsilon}_n = n$ (the work hardening rate). These assumptions are justifiable and realistic.

The length of the necked or process zone (ρ) at the notch tip, Fig. 2, is given by

$$(\delta - \epsilon_n d)/\rho = \alpha \tag{7}$$

where α is a constant and d has been defined previously as the width of the process zone. d can be estimated from the reduction in thickness of the sheet that takes place during fracture. The reduction in thickness is uniform up to the point of necking, when the thickness is given by

$$t = t_0(1 - \gamma\epsilon_n) \tag{8}$$

where γ, for an isotropic material, lies between the limits $1/2 < \gamma < 1$. Hill's theory of necking [6] predicts that there is no contraction between the notches of the DENT specimen ($\gamma = 1$), whereas if the notches do not constrain the plastic flow at all, then free contraction occurs ($\gamma = 1/2$). Measurements of the contraction between the notches suggest that γ is nearer one than a half. It is assumed that the neck can be modelled by a trapezoid (see Fig. 3) and that during necking there is contraction between the notches (in either the DENT or shallow-edge notches specimen). Thus the constancy of volume condition gives

$$d = \frac{\delta_c[t_0(1 - \gamma\epsilon_n) + t_n]}{[t_0(1 + \gamma\epsilon_n) - t_n]}. \tag{9}$$

Some simple calculations for a range of thin sheet metals show that d is of the order of magnitude as t_0.

Since the process zone represents a region where unloading takes place, only the material between the process zones undergoes further plastic deformation upon loading. Assuming that at the centre of the ligament the straining is uniform, the increment is given by (see Fig. 2a)

$$d\epsilon_0 = de/(l - 2\rho) \tag{10}$$

where l is the ligament length. Before a crack initiates, Equations 7 and 10 can be combined to give

$$\frac{d\epsilon_0}{de} = \left[l - \frac{2(e - \epsilon_n d)}{\alpha}\right]^{-1} \tag{11}$$

which can be solved using the boundary conditions: $e = \epsilon_n d$ when $\epsilon_0 = e/l = \epsilon_n(d/l)$ to give

$$e - \epsilon_n d = \frac{l\alpha}{2}\left\{1 - \exp\left[-\frac{2}{\alpha}\left(\epsilon_0 - \frac{\epsilon_n d}{l}\right)\right]\right\} \tag{12}$$

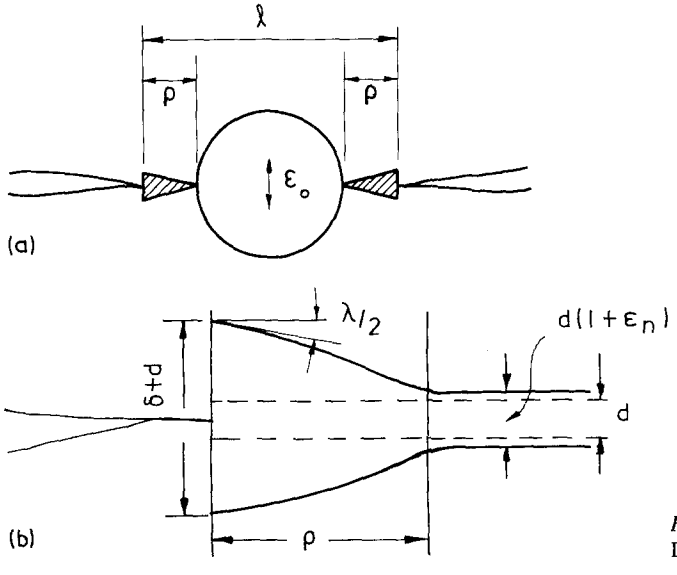

Figure 2 (a) Deformation within the ligament region. (b) Deformation details of the fracture process zone.

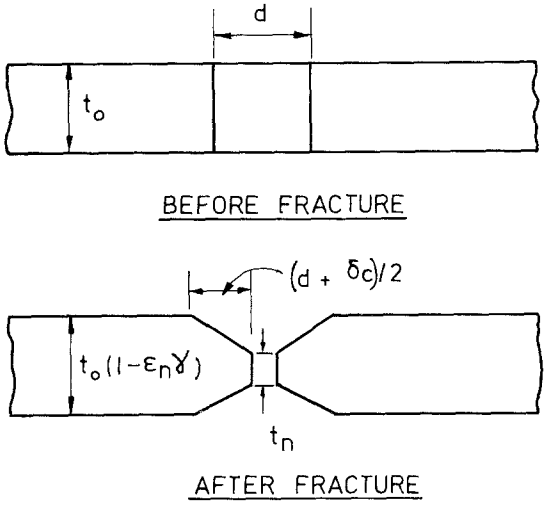

Figure 3 Trapezoidal deformation model used to determine the width of the process zone (d).

which can be rewritten as

$$\epsilon_0 = \frac{\epsilon_n d}{l} - \frac{\alpha}{2} \ln \left(1 - \frac{2\rho}{l}\right). \quad (13)$$

If the ligament is large enough, the process zone develops to its critical length ρ_c at initiation when $e = \delta_c$. However, for small ligaments Equation 13 is invalid when $\rho = \rho_c$ because $\epsilon_0 > \epsilon_n$ and smooth development of the process zone can only occur for $\epsilon_0 < \epsilon_n$. When $\epsilon_0 = \epsilon_n$ the whole ligament is on the point of incipient necking and the elongation given by Equation 12 is

$$e = \frac{l\alpha}{2}\left\{1 - \exp\left[-\frac{2\epsilon_n}{\alpha}\left(1 - \frac{d}{l}\right)\right]\right\} \quad (14)$$

The total elongation (e_t) of the DENT specimen at fracture may be estimated as follows. Consider first the case where the ligament is large. After crack initiation, at $e = \delta_c$, the crack propagates incrementally towards the centre of the ligament increasing ϵ_0. The ligament length (l^*) at which $\epsilon_0 = \epsilon_n$ can be obtained from Equation 13 for $\rho = \rho_c$ and is given by*

$$\epsilon_n(1 - d/l^*) = -\alpha/2 \ln (1 - 2\rho_c/l^*). \quad (15)$$

It is assumed that the crack opening displacement at the tip of the propagating crack is constant and equal to δ_c and that the shape of the fracture process zone does not change. Thus, if the slope of the process zone at the crack tip is defined by λ (see Fig. 2b) it is necessary to stretch the specimen by an amount λda in order to produce a crack extension da. Thus, the specimen has to be stretched by $\lambda/2(l - l^*)$ in order to propagate the cracks until the ligament has decreased to l^*. After necking is established throughout the ligament, a further elongation of $(\delta_c - \epsilon_n d)$ fractures the remaining ligament (l^*). This assumption is justified since experiments in the α-brass specimens with very shallow blunt notches show that the elongation from maximum load to fracture is very close to $(\delta_c - \epsilon_n d)$. This observation is also found to be true for a range of other thin ductile metal sheets. Thus,

$$e_t = 2\delta_c + \lambda/2(l - l^*) - \epsilon_n d \quad (16)$$

and λ can be obtained from the slope of the e_t versus l plot.

When $l < l^*$, e_t is the sum of Equation 14 and $(\delta_c - \epsilon_n d)$, i.e.

$$e_t = \delta_c + \frac{\alpha l}{2}\left\{1 - \exp\left[\frac{-2}{\alpha}\epsilon_n(1 - d/l)\right]\right\} \quad (17)$$

3.2. Effect of pre-strain on critical crack opening displacement and elongation to fracture

When the DENT specimens have been pre-strained by an amount ϵ_s, they may be considered as having received a prior stretching of $\epsilon_s d$ so that the critical opening displacement at crack initiation ($_s\delta_c$) is reduced to

$$_s\delta_c = \delta_c - \epsilon_s d. \quad (18)$$

Similarly the elongation to fracture becomes

$$_se_t = 2\delta_c + \lambda_s/2(l - l_s^*) - (\epsilon_n + \epsilon_s)d \quad (19)$$

for $l > l_s^*$ and

$$_se_t = \delta_c + \frac{\alpha_s l}{2}\left\{1 - \exp\left[\frac{-2}{\alpha_s}\epsilon_n(1 - d/l)\right]\right\} - \epsilon_s d \quad (20)$$

for $l < l_s^*$. The subscript s in α, λ and l^* refer to the pre-strained material. α_s can be obtained from Equation 7 with $\delta = \delta_c$ and $\rho = {}_s\rho_c$ (the process zone size for the pre-strained specimens). It has

* It is shown in [5] that an exact expression for l^* is given by: $l^* = 2\rho_c + l(1 - 2\rho_c/l)^{1 - \alpha/\lambda} \exp[-2\epsilon_n/\lambda(1 - d/l)]$. This means that l^* is dependent on l. However for the range of ligaments used in this work the above expression and Equation 15 both give similar l^* values for all the pre-strained and as-received specimens.

been experimentally observed that ${}_s\rho_c$ increases with increasing ϵ_s (see Table II later). It is assumed that the slope of the process zone λ at the crack tip is proportional to α and that $(\delta_c - \epsilon_n d)$ is independent of the pre-strain. Thus

$$\lambda/\lambda_s = \alpha/\alpha_s = {}_s\rho_c/\rho_c. \quad (21)$$

l_s^* may be obtained by solving Equation 15 knowing α_s and ${}_s\rho_c$.

3.3. Partitions of the specific work of fracture

The specific work of fracture (w_f) in the DENT specimens can be obtained by dividing the work area under the load–displacement curve with the ligament area. In our previous work [3, 4], it is stated that the intercept of the w_f versus l plot gives the specific essential work of fracture (w_e). This is only true if $2\rho_c \ll l$ such as in low alloy steel [3] and in Lyten [4]. A more detailed analysis [5] shows that w_f can be partitioned into four work components, two for the crack initiation phase and two for the propagation phase. Thus,

$$w_f = w_i^e + w_i^p + w_p^p + w_p^e \quad (22)$$

where $w_e = w_i^e + w_p^e$ the specific essential work. The subscripts i and p denote initiation and propagation respectively and the superscripts e and p the essential and non-essential plastic work. Fig. 4 shows schematically how the various components of w_f vary with l. Note that $w_i = (w_i^e + w_i^p)$ is independent of l and that $w_i = w_e$. At large l, w_p^e becomes equal to w_e and w_i^e becomes zero.

4. Experimental work

The material used in this work was a 1.02 mm thick commercial α-brass Austral 207 with 30% zinc and negligible amounts of lead and silver. In the transverse direction the yield stress is 200 MPa, the ultimate tensile strength is 330 MPa and the elongation to break on 50 mm gauge length is approximately 50%. The true stress–true strain relation was obtained as follows

$$\bar{\sigma} = 625\,\bar{\epsilon}^{0.32}. \quad (23)$$

Rectangular specimens of dimensions 600 mm × 100 mm were cut from the sheet metal such that the loading was transverse to the rolled direction. Pre-strains were applied to these specimens by stretching them uniformly to predetermined amounts of 5, 10, 15, 20, 25 and 35% respectively. Fig. 5 shows the variation of yield strength, microhardness and elongation to break with ϵ_s. Edge notches were finally introduced midway on the long sides of the as-received and pre-strained specimens so that a range of ligament lengths from 5 to 30 mm was obtained. The last few millimeters of the notches were finished with a 0.15 mm thick blade. These specimens were then fractured in the Shimadzu machine and the load–elongation curves recorded autographically with an X–Y recorder. The elongation at the centre of the ligament was

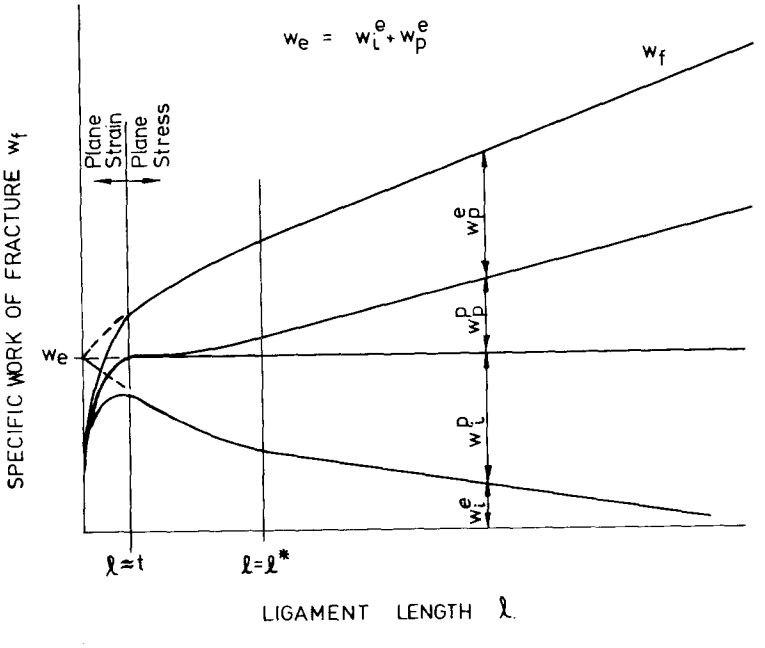

Figure 4 Partitions of the total specific work of fracture and their variation with ligament length.

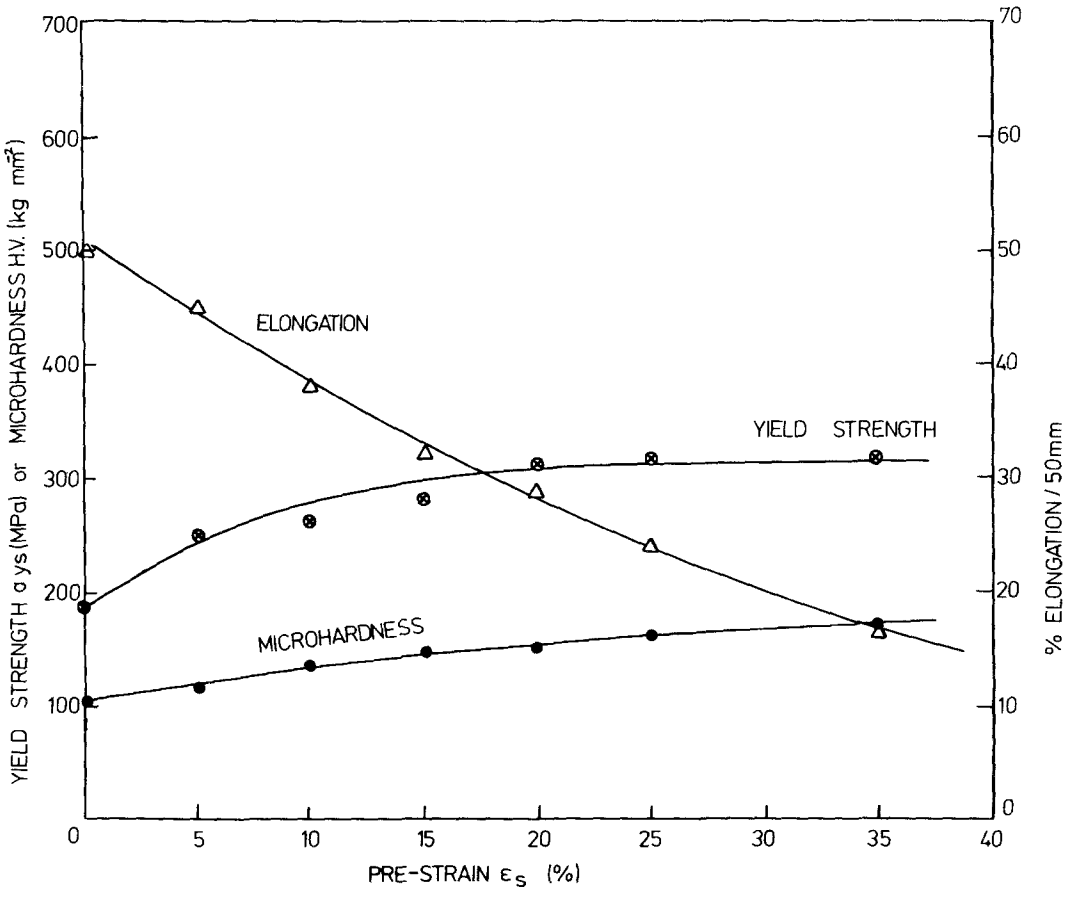

Figure 5 Variation of yield strength, elongation to break and micro-hardness for the as-received and pre-strained specimens.

measured over a gauge length of 120 mm with two clip gauges one on each side of the specimen. The plastic elongation at which the crack was initiated at the notch tip was also observed and marked off on the load–elongation record.

Since strain localization near the fracture edge was thought to affect the critical crack opening displacement [1] micro-hardness measurements were taken on properly prepared samples cut from the fractured DENT specimens with and without pre-strains. In addition strain localization within the fracture process zone was studied on DENT samples with cracks just initiated at the notches. These results together with micro-hardness measurements just outside the neck of tensile specimens provide an experimental method to determine the fracture process zone size. The Shimadzu micro-hardness tester with a load of 50 g and an indentation time of 15 sec was used.

5. Results and discussions

5.1. Effect of pre-strain on strain localization

The strain localization near the fractured edge is given in Fig. 6 in which the microhardness measurements are plotted against the non-dimensional distance (y/l), where y is the distance in the vertical direction measured at the centre of the ligament. The non-dimensional distance is preferred since this allows microhardness results of different ligament lengths to be plotted on the same graph. It is clear from these results, Fig. 6, that the strains become increasingly localized at the fracture surface as the pre-strain levels are raised. It may thus be argued that these highly localized strains are largely responsible for the low values of ${}_sw_e$ and ${}_s\delta_c$ obtained in the pre-strain specimens. There are two other interesting features of these experimental results. Firstly, the strain near the

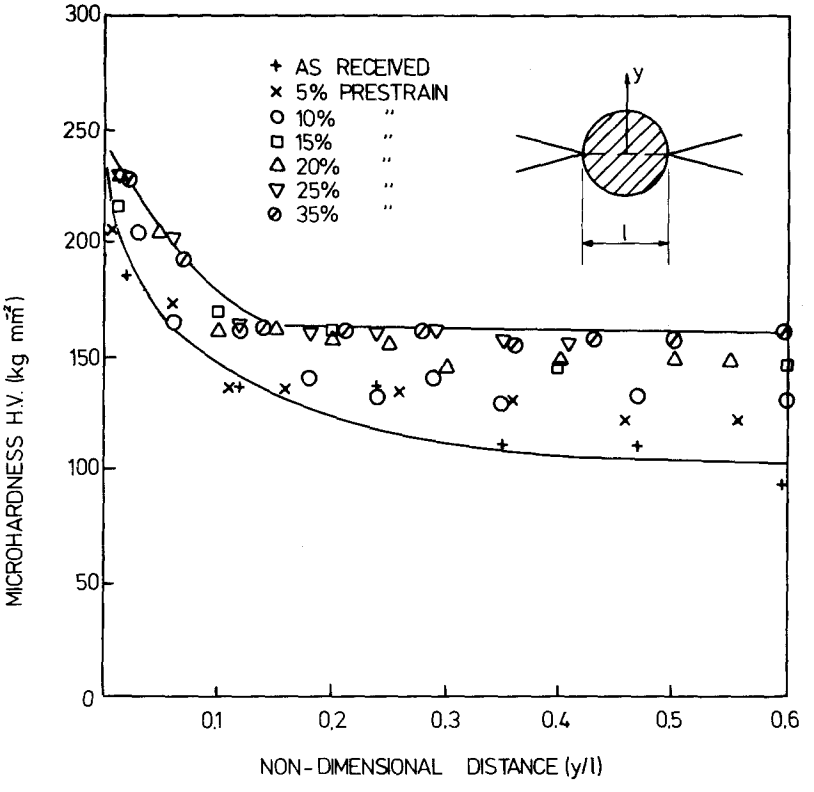

Figure 6 Strain localization near fractured surface for as-received and pre-strained specimens.

fractured edge, i.e. $y/l \to 0$, is approximately the same for all specimens, whether as-received or pre-strained. This confirms the idea that the total strain, i.e. pre-strain (if any) plus strain up to necking and additional strain to break the neck, experienced by the material at fracture must be the same. Table I gives the fracture strain in terms of microhardness for varying pre-strain levels. The matrix hardness values are also provided for comparative purposes. Secondly, the microhardness levels out at $y/l \approx 0.50$ to their respective matrix hardness values for the as-received and pre-strained specimens with ϵ_s less than 20%. These results justify Equation 10 in assuming a circular plastic deformation zone in the ligament region. However for $\epsilon_s > 20\%$ the microhardness levels out to the matrix values at $y/l \approx 0.2$ and this suggests that a constant equal to 5 should be put on the right hand side of Equation 10. The effect of this constant in determining the elongation to fracture (e_t) is discussed in Section 5.3.

TABLE I Micro-hardness measurements for α-brass specimens with varying pre-strain levels

Condition	Micro-hardness, HV (kg mm^{-2})	
	Matrix*	Near fracture edge
As-received	100 ± 4 (8)†	232 ± 6 (8)
5% pre-strain	116 ± 4 (8)	216 ± 9 (8)
10% pre-strain	134 ± 5 (10)	217 ± 9 (10)
15% pre-strain	143 ± 6 (4)	227 ± 7 (4)
20% pre-strain	148 ± 4 (6)	228 ± 6 (6)
25% pre-strain	158 ± 5 (8)	223 ± 10 (8)
35% pre-strain	163 ± 5 (8)	224 ± 8 (8)

* 1 standard deviation is given.
† Number in bracket indicates number of measurements taken.

Strain localization within the fracture process zone is shown in Fig. 7 where microhardness is plotted against distance from the crack tip (x). The dashed line represents the average microhardness (H.V. = 180 kg mm^{-2}) of the material just outside of the neck in a tensile specimen and this value is found to be the same for the as-received and pre-strained specimens. It is suggested that the intersections of this line and the strain localization curves define the size of the process zone. This criterion is thought to be reasonable, because at the tip of the process zone the local strain must be equal to ϵ_n. As shown in Table II the process zone size increases with increasing amounts of pre-strain. The microhardness at the tip of the notch with an initiated crack is again independent of pre-strain and has a value close to that given in Fig. 6.

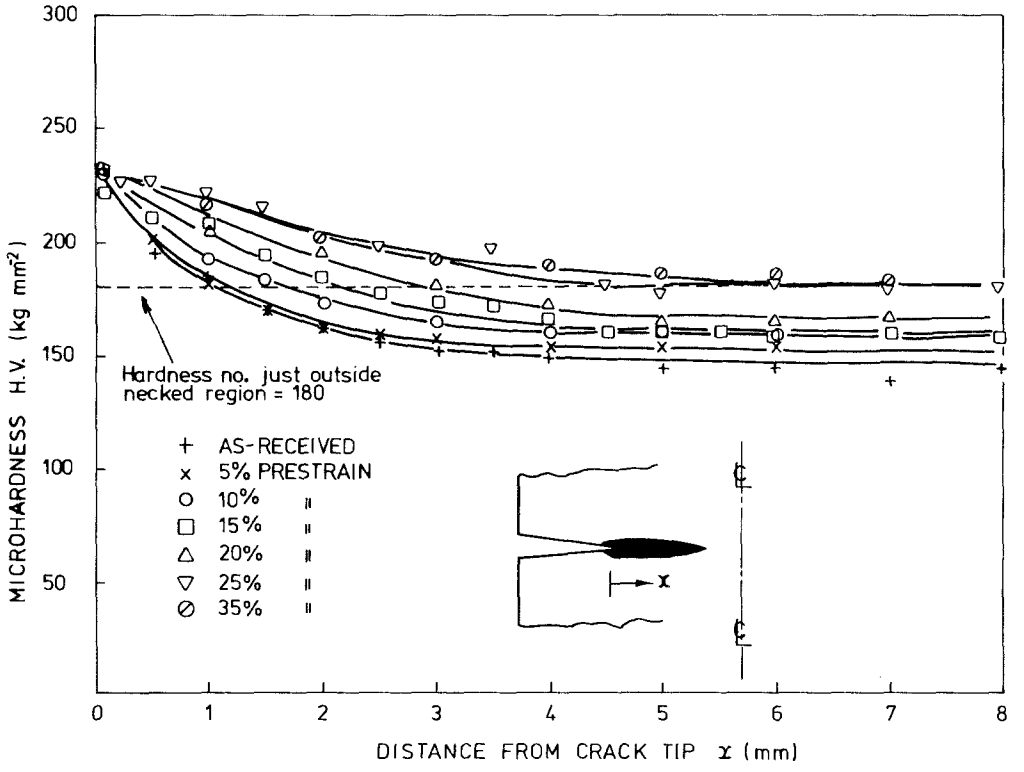

Figure 7 Strain distribution within the fracture process zone as a function of distance from crack tip.

5.2. Specific essential work of fracture results

A summary of all the specific work of fracture results, w_i and w_f, are shown in Fig. 8. As discussed in Section 3.3 and graphically illustrated in Fig. 4, $w_i = w_e$ when $l \to 0$. Note that w_i does not depend on l, however, it does decrease with increasing pre-strain. The total specific work of fracture (w_f) least square lines appear to give the same intercept on the y-axis, i.e. $\sim 260\,\mathrm{kJ\,m^{-2}}$, which is the value of w_i and consequently w_e for the as-received specimens. The fact that all the w_f lines give the same intercept value is only fortuitous and should not be taken as to imply w_e is independent of pre-strain. Clearly, w_e $(= w_i)$ decreases as ϵ_s is increased. It is also noted that when $l \leqslant 8$ mm w_f decreases more than the least square lines suggest, probably because $l \approx 2\rho_c$ and the plane strain–plane stress transition occurs at the notch tip for these small ligaments.

Equations 4 and 5 may be used to predict w_e for the as-received and pre-strained materials. The true stress–true strain relation is given by Equation 23, i.e. $\bar{\sigma} = 625\,\bar{\epsilon}^{0.32}$ so that $\bar{\epsilon}_n = 0.32$ and $\epsilon_n = 0.375$. Now experimental results yield $\delta_c = 0.90$ mm (see Section 5.3 later) and $t_n = 0.38$ mm. Thus Equation 9 gives the width of the process zone, $0.90 < d < 1.31$ for $1/2 < \gamma < 1$. It is still

TABLE II Parametric values as a function of pre-strain

Condition	$_s\rho_c$ (mm)	λ_s		α_s		l_s^* (mm)	
		$\gamma = 1/2$	$\gamma = 1$	$\gamma = 1/2$	$\gamma = 1$	$\gamma = 1/2$	$\gamma = 1$
As-received	1.10	0.23	0.23	0.37	0.51	3.20	3.35
5% pre-strain	1.20	0.21	0.21	0.34	0.46	3.30	3.40
10% pre-strain	1.70	0.15	0.15	0.24	0.33	3.90	4.10
15% pre-strain	2.20	0.12	0.12	0.19	0.26	4.70	4.85
20% pre-strain	2.90	0.09	0.09	0.14	0.19	5.90	6.00
25% pre-strain	4.50	0.06	0.06	0.09	0.13	9.00	9.00
35% pre-strain	6.00	0.04	0.04	0.07	0.09	12.00	12.00

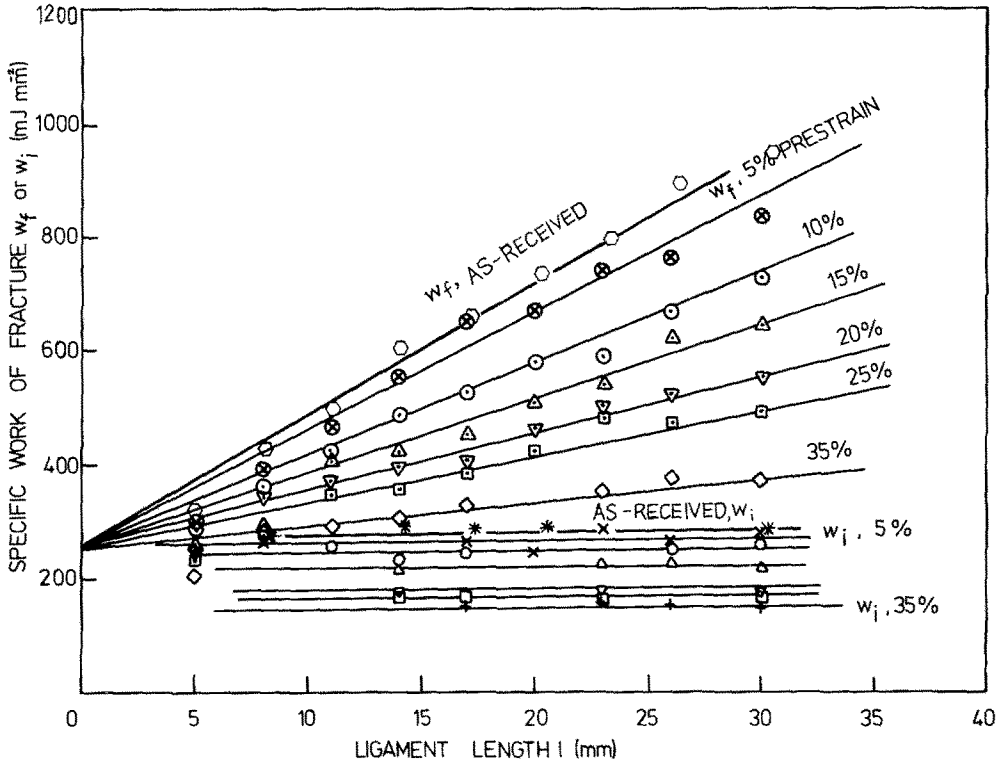

Figure 8 Variation of specific work of fracture, w_f and w_i, with ligament length (l).

necessary to determine the functional relation between σ and δ after necking is reached. Using tension specimens with shallow blunt notches it was found that σ at necking and σ at crack initiation differed only by approximately 20 MPa so that an average σ value of 310 MPa was assumed constant over the stretched distance (δ) from necking to fracture. Experiments have shown that after necking a further stretch distance equal to $(\delta_c - \epsilon_n d)$ is required to cause fracture irrespective of whether pre-strained or not. Table III compares

TABLE III Comparison of specific essential word of fracture obtained from experiment and predicted by Equations 4 and 5

Condition	Specific Essential work of fracture (kJ m^{-2})		
	Experimental	Prediction $\gamma = 1/2$	$\gamma = 1$
As-received	262*	263	268
$\epsilon_s = 0.05$	250†	251	260
0.10	240	235	249
0.15	220	216	236
0.20	195	197	222
0.25	170	176	208
0.35	150	136	180

* Least square line intercept of Fig. 8.
† Average w_i values obtained from Fig. 8.

the experimental specific essential work measurements for all the as-received and pre-strained specimens with theoretical predictions. There is good agreement between these results. The reduction in the specific essential work of pre-strained specimens comes from the diminished work dissipated up to necking (w_{e1}). It seems to the present authors that w_e for metals with a high work hardening rate, such as brass studied here, are reduced by pre-strain whereas for metals with low work hardening rates, such as aluminium alloy AA2S and low alloy steel Lyten, w_e is not significantly affected by any amounts of pre-strain.

5.3. Critical crack opening displacement and elongation to fracture results

The critical crack opening displacement (δ_c) in the as-received specimens was found to be 0.90 mm being independent of ligament size. Using Equation 18 and $d = 0.90$ and 1.31 mm respectively, it is possible to calculate the critical crack opening displacements for the pre-strained specimens. As shown in Table IV the experimental ${}_s\delta_c$ values agree reasonably well with theoretical predictions for $\gamma = 1/2$. For $\gamma = 1$ and $\epsilon_s > 0.20$, the agreement however is poor.

TABLE IV Comparison of experimental crack tip opening displacement with predictions by Equation 18

Condition	Critical crack tip opening displacement (mm)		
	Experimental	Prediction	
		$\gamma = 1/2$	$\gamma = 1$
As-received	0.90	–	–
$\epsilon_s = 0.05$	0.90 ± 0.01*	0.84	0.86
0.10	0.71 ± 0.04	0.77	0.81
0.15	0.67 ± 0.02	0.71	0.76
0.20	0.52 ± 0.02	0.64	0.72
0.25	0.41 ± 0.02	0.57	0.67
0.35	0.34 ± 0.02	0.44	0.58

* 1 standard deviation is given and a sample size of 5 is used over a range of ligament lengths.

Fig. 9 shows the elongation to fracture (e_t) plotted against l. It is interesting to see if the simple deformation theory given in Section 2 can be used to predict the variation of e_t with ϵ_s, i.e. Equations 19 and 20. To start with α and λ have to be determined for the as-received material using Equations 7 and 16 e.g. for $d = 1.31$ mm, $\alpha = (\delta_c - \epsilon_n d)/\rho_c = (0.90 - 0.375 \times 1.31)/1.1 = 0.37$ and λ is obtained from the slope of the least square line shown in Fig. 9, which gives $\lambda = 0.23$. Equations 15 and 21 then allow l_s^*, α_s and λ_s to be obtained as a function of ϵ_s. These theoretical lines are superimposed in Fig. 9 and comparison with experimental results shows good agreement for $\gamma = 1/2$ and $\epsilon_s \leqslant 0.20$. The agreement becomes poor for any single γ and the complete range of ligament lengths (l) when $\epsilon_s = 0.25$ and 0.35. However these experimental data are bounded by the theoretical lines for $\gamma = 1/2$ and 1.

It was initially thought that the intense strain localization for the highly pre-strained specimens, e.g. $\epsilon_s = 0.25$ and 0.35, as discussed in Section 5.1 could have affected to a certain degree predictions for e_t. If Equation 10 is adjusted with a constant equal to 5 the left hand side of Equation 15 becomes $\epsilon_n(1/5 - d/l^*)$. This gives $l_s^* \approx 17$ mm and 18 mm for $\epsilon_s = 0.25$ and 0.35 respectively and the intercept values of the resultant e_t equations are now reduced by 20% and 40% respectively. The agreement between these results is worse. In fact the elongation to fracture predictions for these

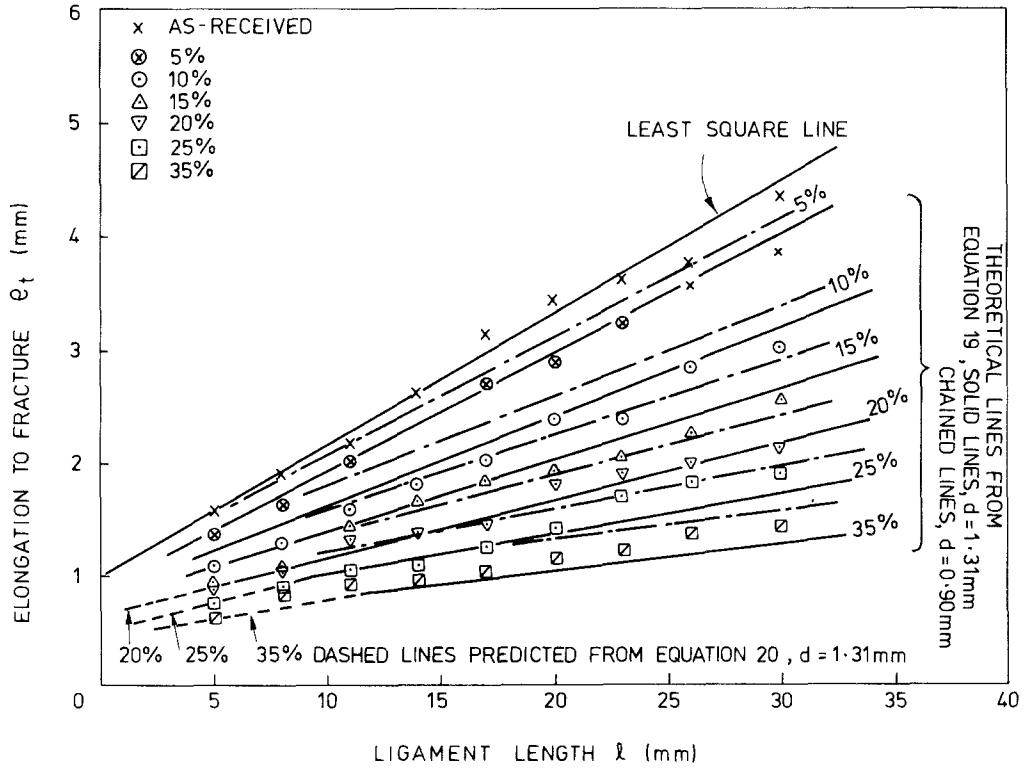

Figure 9 A plot of elongation to fracture (e_t) versus ligament length (l). Theoretical lines for $d = 1.31$ mm and $\gamma = 1/2$, $d = 0.90$ mm and $\gamma = 1$.

highly pre-strained specimens are more sensitive to changes in λ_s, which is reflected by the sensitivity in determining ${}_s\rho_c$ from Fig. 7.

6. Conclusions

The effects of pre-strain on the plane stress ductile fracture behaviour of an α-brass have been studied in the present paper. It was found that the specific essential work of fracture (${}_sw_e$) decreased as the amounts of pre-strain were increased. This was a consequence of the reduction of plastic work absorbed up to necking as given by Equation 5. Strain localization was more intense near the fracture surface when ϵ_s was large. The simple deformation theory presented for the DENT specimens predicted elongation to fracture (e_t) values in reasonably good agreement with experimental results. The crack opening displacement at initiation was also found to decrease with increasing pre-strain as predicted by Equation 18. It is concluded that in general pre-strains have more effects in reducing w_e and δ_c in metals with high work hardening rates than metals with low work hardening rates.

Acknowledgements

The authors wish to thank the Australian Research Grants Committee and the Sydney University Research Grants Committee for supporting the work reported in this paper. The technical assistance provided by Mr. S. R. Errey is appreciated.

References

1. G. GREEN, R. F. SMITH and J. F. KNOTT, "Metallurgical Factors in Low Temperature Slow Crack Growth", British Steel Corporation Conference on the Mechanics and Mechanisms of Crack Growth, Cambridge, April, 1973. Paper 5.
2. J. D. G. GROOM and J. F. KNOTT, "Effects of Pre-strain on Ductile Fracture", First International Conference on Mechanical Behaviour of Materials, Kyoto, Japan, 1971. Vol. 1, pp. 265–275.
3. Y. W. MAI and K. M. PILKO, *J. Mater. Sci.* **14** (1979) 386.
4. B. COTTERELL and J. K. REDDEL, *Int. J. Fracture*, **13** (1977) 267.
5. B. COTTERELL and Y. W. MAI, to be presented at the Fifth International Conference on Fracture, Cannes, France, 1981.
6. R. HILL, *J. Mech. and Phys. Solids* **1** (1952) 19.

Received 12 December 1979 and accepted 5 February 1980.